

SUPPORTING INFORMATION

Separation of Precise Compositions of Noble Metal Clusters Protected with Mixed Ligands

Yoshiki Niihori,^a Miku Matsuzaki,^a Thalappil Pradeep,^{*b} and Yuichi Negishi,^{*a}

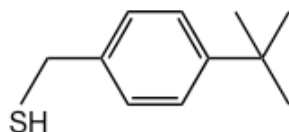
^a Department of Applied Chemistry, Faculty of Science, Tokyo University of Science, 1-3 Kagurazaka, Shinjuku-ku, Tokyo 162-8601, Japan. ^b DST Unit of Nanoscience (DST UNS) and Thematic Unit of Excellence, Indian Institute of Technology Madras, Chennai 600 036, India.

Supporting Information I

Experimental Methods

A. Chemicals

All chemicals were obtained commercially and used without further purification. Hydrogen tetrachloroaurate tetrahydrate (HAuCl₄·4H₂O) was obtained from Tanaka Kikinzoku. Palladium sodium chloride trihydride (Na₂PdCl₄·3H₂O), tetraoctylammonium bromide ((C₈H₁₇)₄NBr), sodium tetrahydroborate (NaBH₄), hexanethiol (C₆H₁₃SH), decanethiol (C₁₀H₂₁SH), dodecanethiol (C₁₂H₂₅SH), hexadecanethiol (C₁₆H₃₃SH), methanol (CH₃OH), acetone, toluene, dichloromethane (CH₂Cl₂), and tetrahydrofuran (THF) were obtained from Wako Pure Chemical Industries. 2-Phenylethanethiol (PhC₂H₄SH) was purchased from Tokyo Kasei. The 4-(*tert*-butyl)benzyl mercaptan (BBSH, Scheme S1) were purchased from Aldrich. The matrix, *trans*-2-[3-(4-*tert*-butylphenyl)-2-methyl-2-propenylidene] malononitrile (DCTB) was purchased from Fluka. Deionized water with a resistivity > 18.2 MΩ cm was used.



Scheme S1 Molecular structure of 4-(*tert*-butyl)benzyl mercaptan (BBSH)

B. Synthesis of PdAu₂₄(SC₁₂H₂₅)₁₈, Au₂₅(SC₁₂H₂₅)₁₈, and Au₃₈(SC₁₂H₂₅)₂₄

PdAu₂₄(SC₁₂H₂₅)₁₈ (Fig. S1(a)), Au₂₅(SC₁₂H₂₅)₁₈ (Fig. S1(b)) and Au₃₈(SC₁₂H₂₅)₂₄ (Fig. S1(c)) were synthesized by methods reported previously.¹⁻³

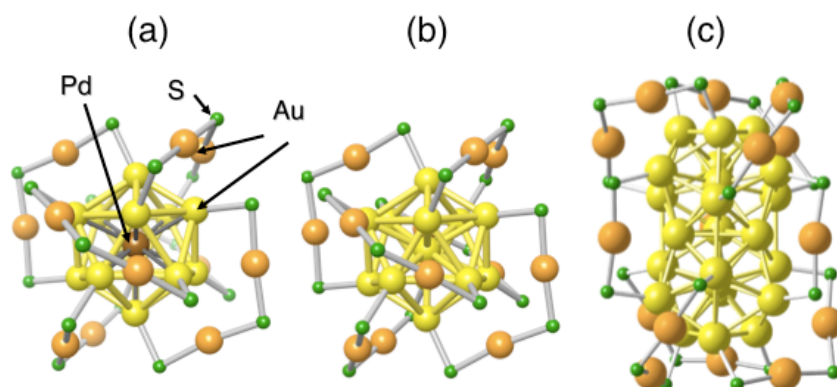


Figure S1. Structural representation of thiolate-protected metal clusters; (a) PdAu₂₄(SR)₁₈ (Ref. 1); (b) Au₂₅(SR)₁₈ (Refs. 4 and 5); and (c) Au₃₈(SR)₂₄ (Ref. 6) (The R moieties are omitted for clarity.)

C. Ligand exchange reactions

An amount of 0.14 μmol of $\text{PdAu}_{24}(\text{SC}_{12}\text{H}_{25})_{18}$, $\text{Au}_{25}(\text{SC}_{12}\text{H}_{25})_{18}$, or $\text{Au}_{38}(\text{SC}_{12}\text{H}_{25})_{24}$ was dissolved in 500 μL of dichloromethane. To this solution, 140 μmol of BBSH, $\text{C}_n\text{H}_{2n+1}\text{SH}$ ($n = 6, 10, \text{ or } 16$), or $\text{PhC}_2\text{H}_4\text{SH}$ was added and the solution was stirred at room temperature. The reaction was stopped at specific time duration. The solution was washed with a mixture of methanol and water to remove excess thiols, and the product was characterized by matrix-assisted laser desorption-ionization (MALDI) mass spectrometry. The PdAu_{24} , Au_{25} , or Au_{38} clusters with various chemical compositions were synthesized by changing the reaction time.⁷

D. HPLC experiments using a reverse-phase column

HPLC experiments were conducted on a Shimadzu instrument consisting of a CBM-20A controller, DGU-20AR on-line degasser, LC-20AD pump, SIL-20A auto-sampler, CTO-20A column oven, and SPD-M20A photodiode array (PDA) detector at IIT Madras or a Waters instrument consisting of a 600E controller, 486 tunable absorption detector, and 625 pump at Tokyo University of Science. The stainless steel column (250 \times 4.6 mm i.d.) packed with 5- μm C18 bonded silica with 300- \AA pore size (Theromo Scientific) was used as the reverse-phase column. This column is suitable for the separation of molecules with different polarity and is different from that used by Bürgi *et al.* for the separation of enantiomers of $\text{Au}_{38}(\text{SC}_2\text{H}_4\text{Ph})_{24}$ (Refs. 8-10). Column temperature was 25 $^\circ\text{C}$. The absorbance chromatogram was monitored by the PDA at 380 nm. The absorption spectra of the eluted peaks were collected over 190–800 nm by the PDA. Each sample was first diluted in THF (0.1 mg/5 μL) and then suspended in solution by adding 45 μL of CH_3OH . Then, 40 μL of the sample suspension was injected into the instrument with a mobile phase of methanol (CH_3OH) at a flow rate of 1 mL/min. After sample injection, the amount of THF in the mobile phase was continuously increased using a gradient program that increased the $[\text{THF}]/[\text{CH}_3\text{OH}]$ ratio of the mobile phase from 0% to 100% (Figure S3). After analysis, the chromatogram was corrected by subtracting the background measured without a sample. Similar experiments were performed with the following two columns; a stainless steel column (250 \times 4.6 mm i.d.) packed with 5- μm C8 bonded silica with 130- \AA pore size (Theromo Scientific), and a stainless steel column (150 \times 4.6 mm i.d.) packed with 5- μm phenyl bonded silica with 130- \AA pore size (Theromo Scientific). However, the separations of the peaks were poorer under these conditions.

D. Characterization of chemical composition

MALDI mass spectra were collected using a linear time-of-flight mass spectrometer (Applied Biosystems, Voyager Linear RD VDA 500) with a nitrogen laser (wavelength: 337 nm). Measurements were also done with a reflectron time-of-flight mass spectrometer (Applied Biosystems, Voyager DE PRO) at IIT Madras. DCTB was used as the matrix.⁸ The cluster-to-matrix ratio was set to be 1:1000.

Supporting Information II

Results

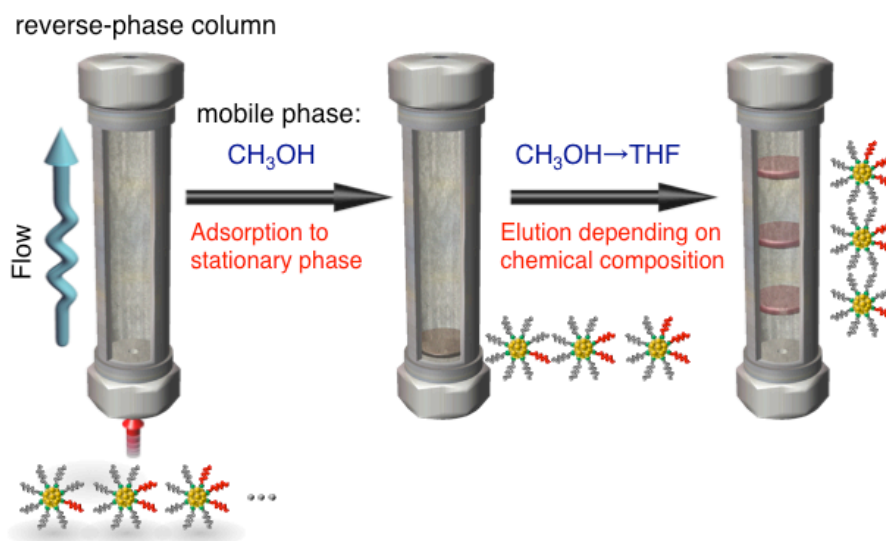


Figure S2. Schematic view of the concept for the high-resolution separation of metal clusters containing two types of thiolates by HPLC involving a reverse-phase column and mobile phase gradient.

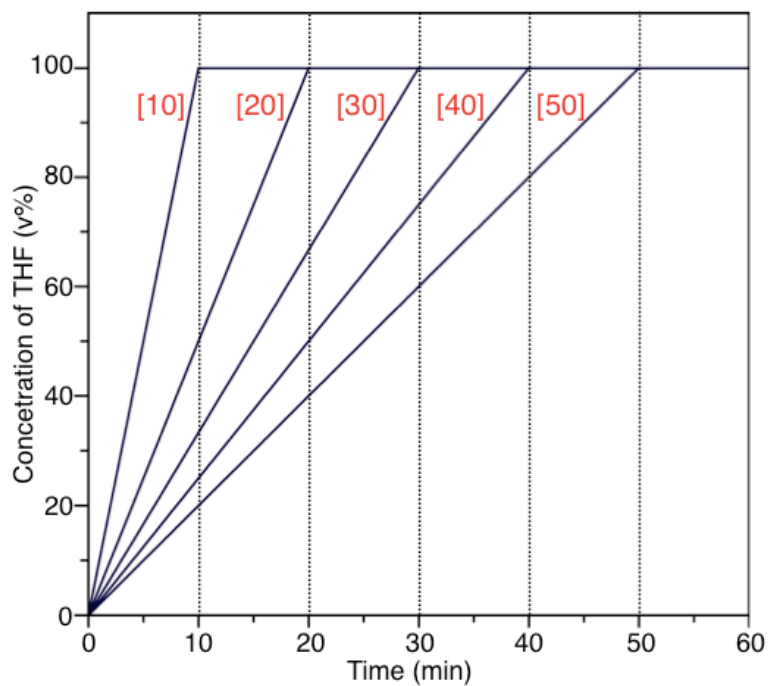


Figure S3. Linear gradient programs used for the high-resolution separation of $\text{PdAu}_{24}(\text{SC}_{12}\text{H}_{25})_{18-n}(\text{SBB})_n$ ($n = 6-16$) (Figure 1(b)). The label (*e.g.*, [10]) in the figure indicates the time (in minutes) taken to fully replace the mobile phase with THF. The program [40] was used as the gradient program for the high-resolution separation for all of the clusters.

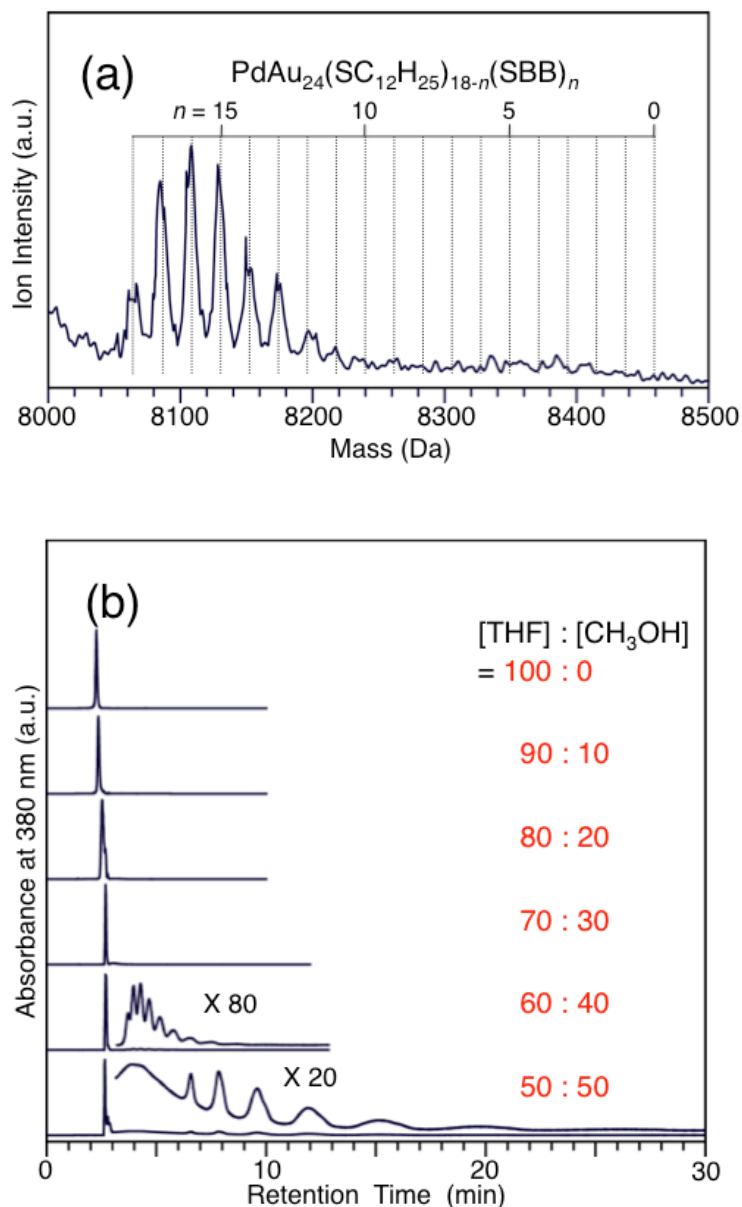


Figure S4. HPLC experiments conducted in an isocratic mode. In these experiments, the mobile phase was fixed to [THF]:[CH₃OH] = 100:0, 90:10, 80:20, 70:30, 60:40, or 50:50. (a) Negative ion MALDI mass spectrum of PdAu₂₄(SC₁₂H₂₅)_{18-n}(SBB)_n ($n = 11-18$) used in these experiments. (b) Chromatograms of PdAu₂₄(SC₁₂H₂₅)_{18-n}(SBB)_n ($n = 11-18$) at each mobile phase. The peaks appearing at 2.3–2.7 min were confirmed to include PdAu₂₄(SC₁₂H₂₅)_{18-n}(SBB)_n ($n = 11-18$). An increase in the concentration of CH₃OH promoted the interaction between PdAu₂₄(SC₁₂H₂₅)_{18-n}(SBB)_n and the stationary phase (column). Therefore, peak separations were observed when the concentration of CH₃OH was increased to 40 and 50 v/v% (enlarged spectra). However, even under those conditions, most of PdAu₂₄(SC₁₂H₂₅)_{18-n}(SBB)_n was not fixed to the stationary phase (column) and was eluted at 2.3–2.7 min. A further increase in concentration of CH₃OH (> 50 v/v%) resulted in the disappearance of the separated peaks. These results indicate that separating all of the clusters is difficult in isocratic mode. Thus, all the clusters must have to be once fixed on the stationary phase for the separation of all the clusters.

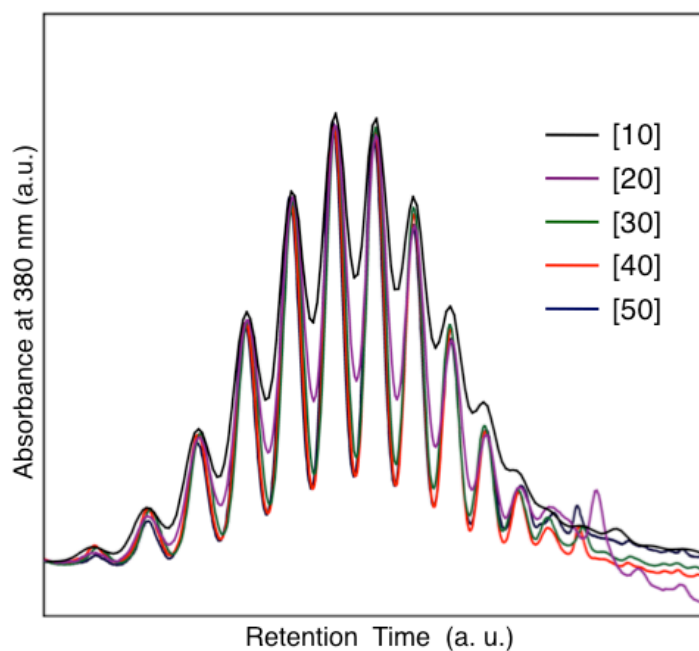


Figure S5. Enlarged chromatograms at each gradient condition. In this figure, the chromatograms are normalized in vertical axis and therefore, the horizontal axis is in arbitrary units. An increase in retention time (Figure 1(b)) resulted in better peak separation under the experimental conditions between [10] and [40]. However, the improvement in resolution was no longer observed at longer retention times (> [40]).

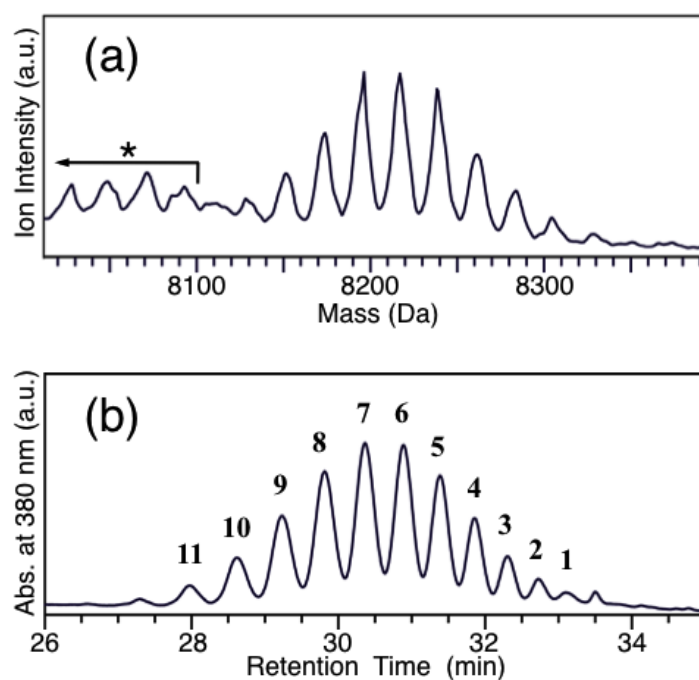


Figure S6. Comparison between the (a) Negative ion MALDI mass spectrum and (b) chromatogram of $\text{PdAu}_{24}(\text{SC}_{12}\text{H}_{25})_{18-n}(\text{SBB})_n$ ($n = 6-16$) (Figure 1(a)). The chromatogram was obtained using a gradient program, [40]. In the mass spectrum, the asterisk indicates the laser fragments.¹¹ The shape of the chromatogram is similar to that of the mass spectrum. Each peak in the chromatogram was fractionated (fractions 1–11) and characterized by MALDI mass spectrometry (see Figure S7).

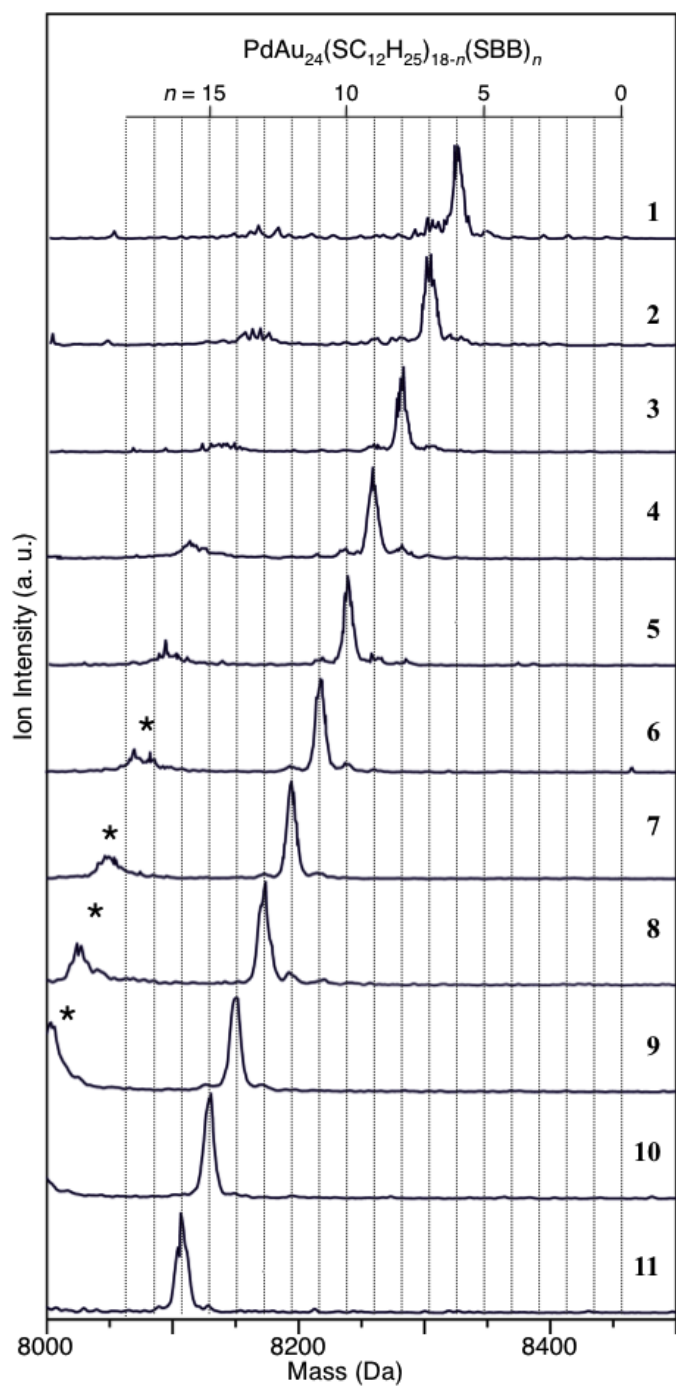


Figure S7. Negative ion MALDI mass spectra of **1–11** (Figure S6(a)). The asterisk indicates the laser fragments. These results indicate that peaks **1–11** contained only a single $\text{PdAu}_{24}(\text{SC}_{12}\text{H}_{25})_{18-n}(\text{SBB})_n$ and that $\text{PdAu}_{24}(\text{SC}_{12}\text{H}_{25})_{18-n}(\text{SBB})_n$ could be separated at high resolution depending on the chemical composition.

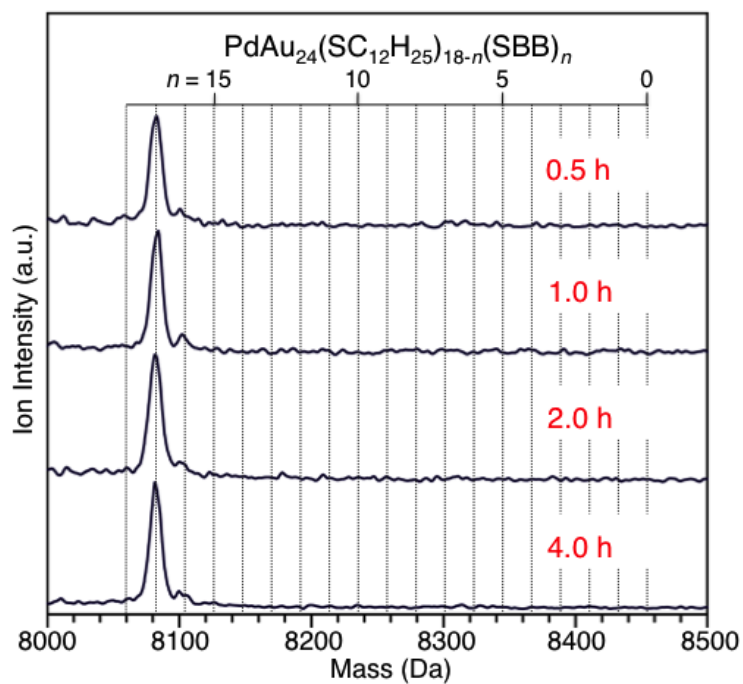


Figure S8. Stability of the isolated $\text{PdAu}_{24}(\text{SC}_{12}\text{H}_{25})(\text{SBB})_{17}$ in CH_2Cl_2 followed by MALDI mass spectrometry. In this experiment, 0.28 mM of $\text{PdAu}_{24}(\text{SC}_{12}\text{H}_{25})(\text{SBB})_{17}$ was diluted in 125 μL of CH_2Cl_2 and left at room temperature. At each time point, a small quantity of the solution was taken and characterized by MALDI mass spectrometry. Results indicated that the isolated $\text{PdAu}_{24}(\text{SC}_{12}\text{H}_{25})(\text{SBB})_{17}$ maintains a chemical composition for at least 4 hours.⁷

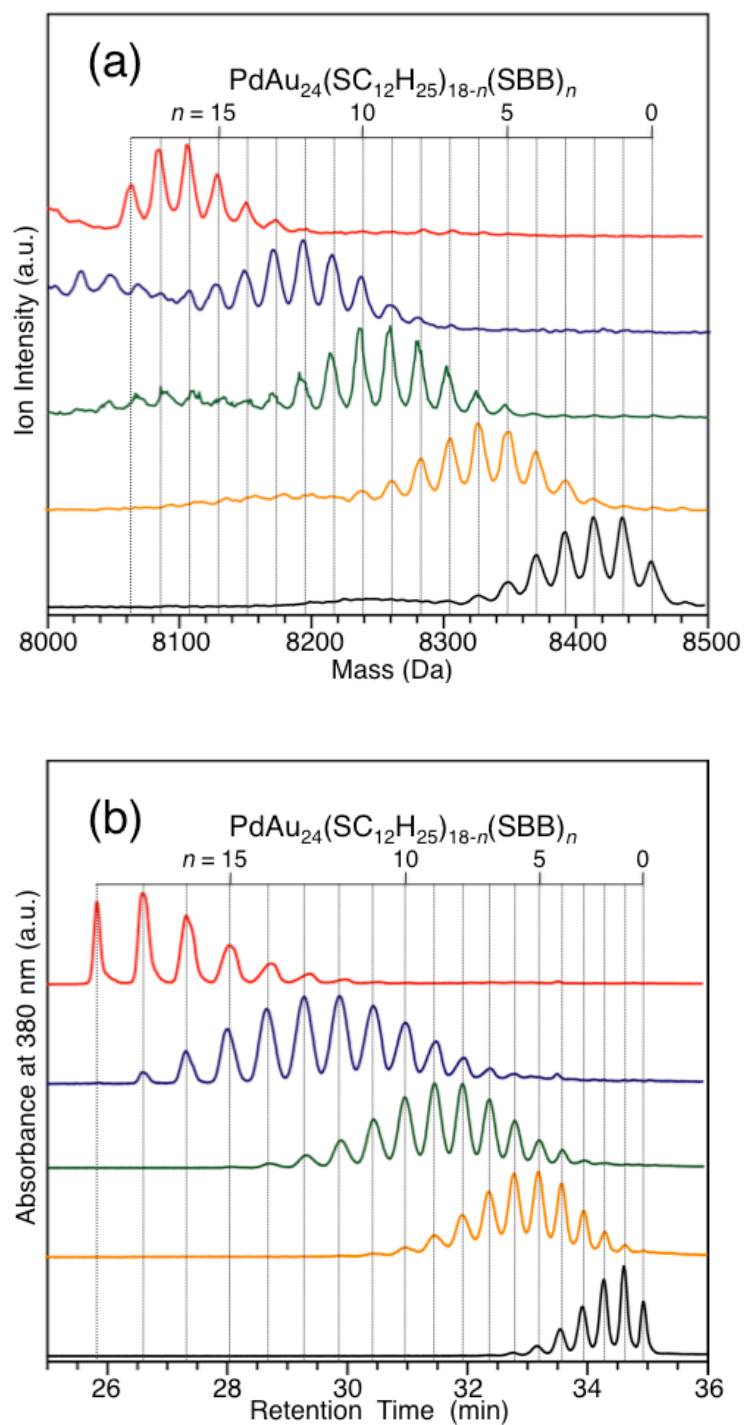


Figure S9. Comparison between (a) Negative ion MALDI mass spectra and (b) chromatograms for $\text{PdAu}_{24}(\text{SC}_{12}\text{H}_{25})_{18-n}(\text{SBB})_n$. The same color indicates the same sample in (a) and (b). A linear gradient program, [40] (Figure S3), was used for these HPLC experiments. In (a), the laser fragment peaks¹¹ also are included (Figures 1(a) and S6(b)). In (b), each peak is labeled with the chemical compositions that were assigned by the mass analysis of each fraction (Figure 2).

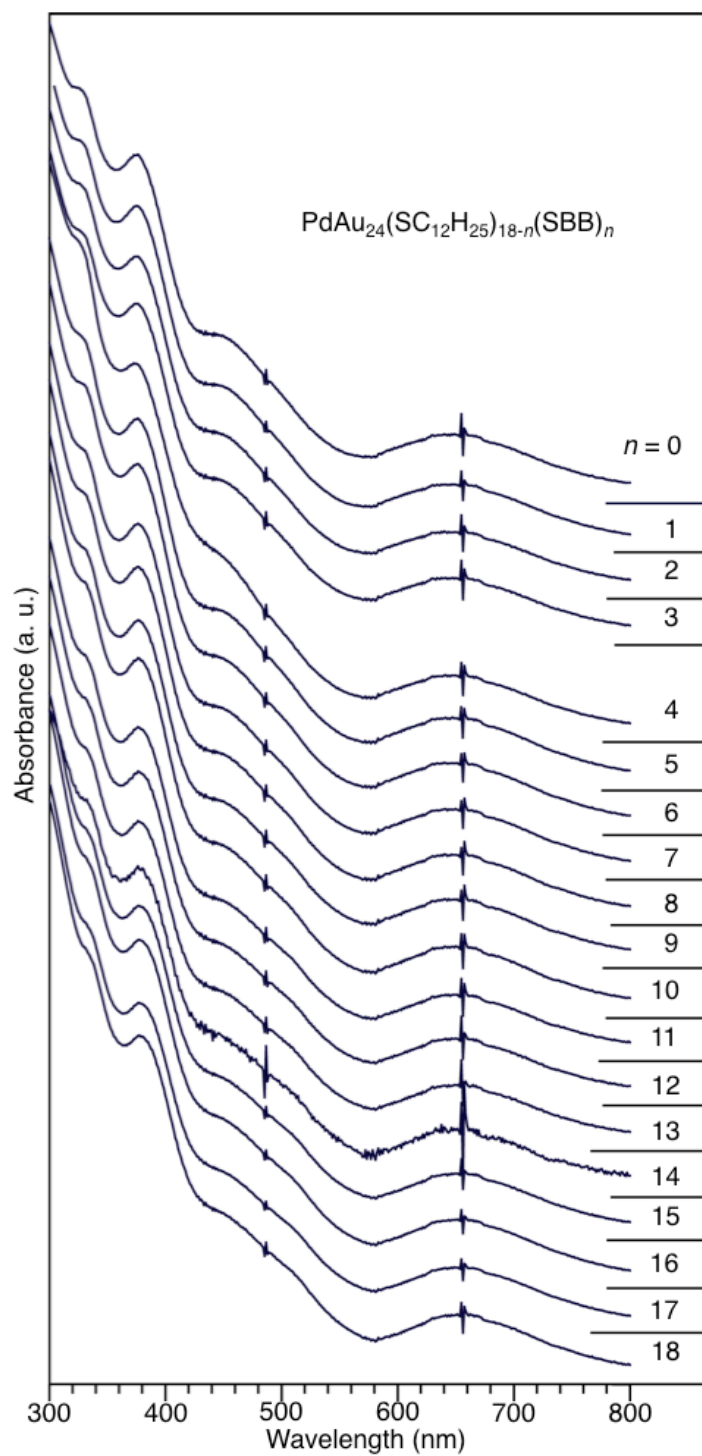


Figure S10. Optical absorption spectra of the isolated $\text{PdAu}_{24}(\text{SC}_{12}\text{H}_{25})_{18-n}(\text{SBB})_n$ ($n = 0-18$) obtained by the PDA detector. All the spectra were normalized at 670 nm. All of the spectra are nearly similar. However, close comparison indicated that the spectral features are slightly different depending on the chemical composition.

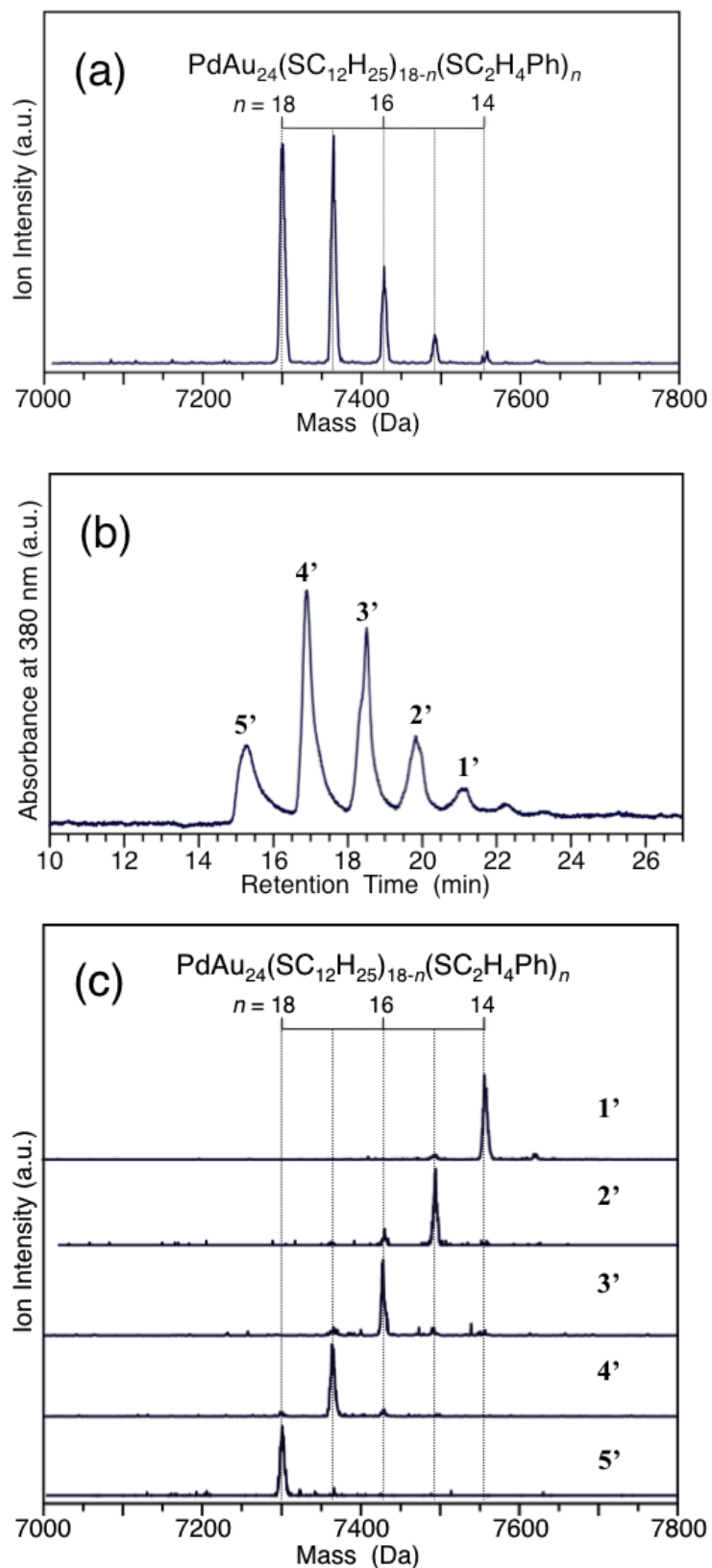


Figure S11. (a) Negative ion MALDI mass spectrum of PdAu₂₄(SC₁₂H₂₅)_{18-n}(SC₂H₄Ph)_n ($n = 14-18$). (b) Chromatograms of these clusters. (c) Negative ion MALDI mass spectra of the fractions of each peak appearing in the chromatogram, 1'-5'. These results indicate that each peak, 1'-5', contains a single PdAu₂₄(SC₁₂H₂₅)_{18-n}(SC₂H₄Ph)_n in high purity and that PdAu₂₄(SC₁₂H₂₅)_{18-n}(SC₂H₄Ph)_n clusters were separated at high resolution depending on the chemical composition.

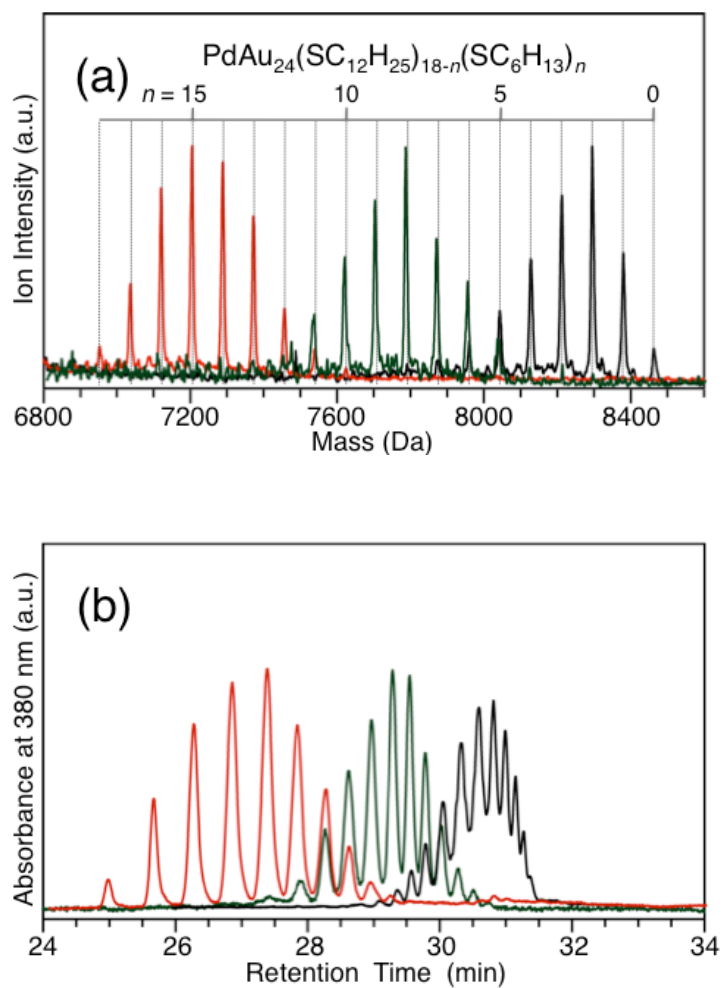


Figure S12. Comparison between the (a) Negative ion MALDI mass spectrum and (b) chromatogram of $\text{PdAu}_{24}(\text{SC}_{12}\text{H}_{25})_{18-n}(\text{SC}_6\text{H}_{13})_n$. In (a) and (b), the same color indicates the same sample. A linear gradient program, [40] (Figure S3), was used for these HPLC experiments.

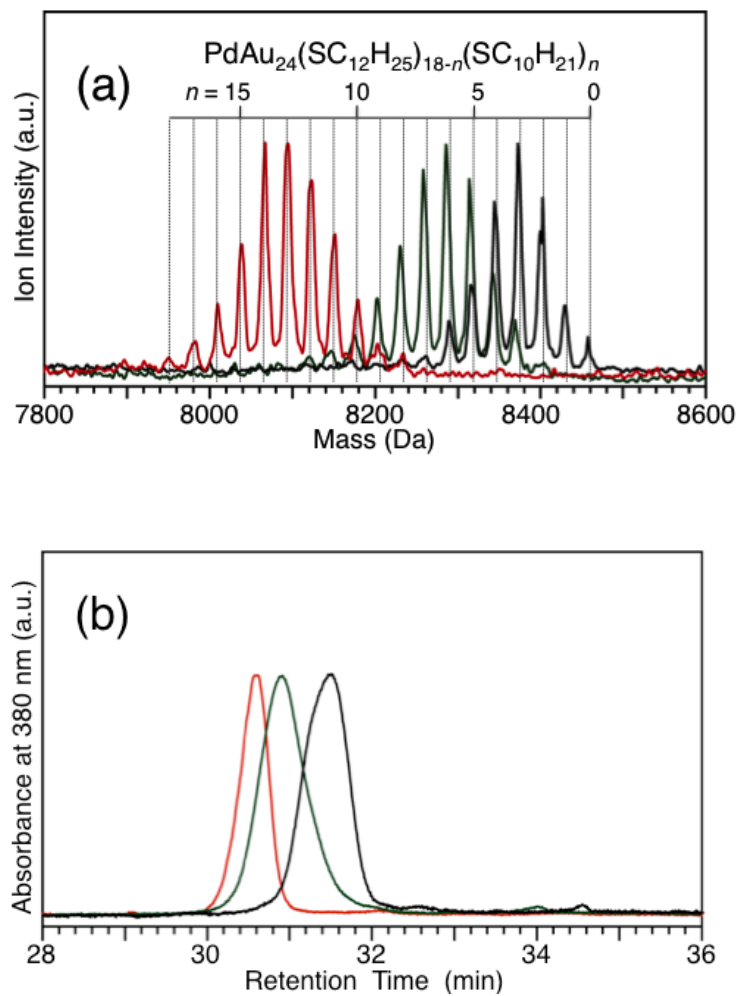


Figure S13. Comparison between the (a) Negative ion MALDI mass spectrum and (b) chromatogram for $\text{PdAu}_{24}(\text{SC}_{12}\text{H}_{25})_{18-n}(\text{SC}_{10}\text{H}_{21})_n$. In (a) and (b), the same color indicates the same sample. A linear gradient program, [40] (Figure S3), was used for these HPLC experiments.

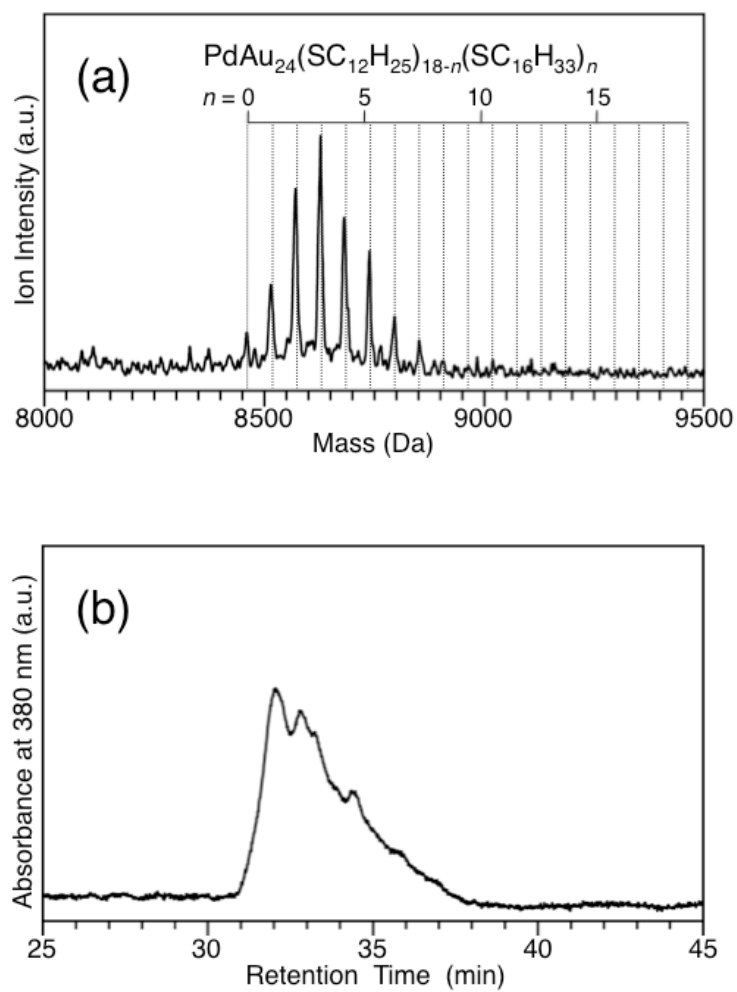


Figure S14. Comparison between the (a) Negative ion MALDI mass spectrum and (b) chromatogram for $\text{PdAu}_{24}(\text{SC}_{12}\text{H}_{25})_{18-n}(\text{SC}_{16}\text{H}_{33})_n$. A linear gradient program, [40] (Figure S3), was used in this HPLC experiment.

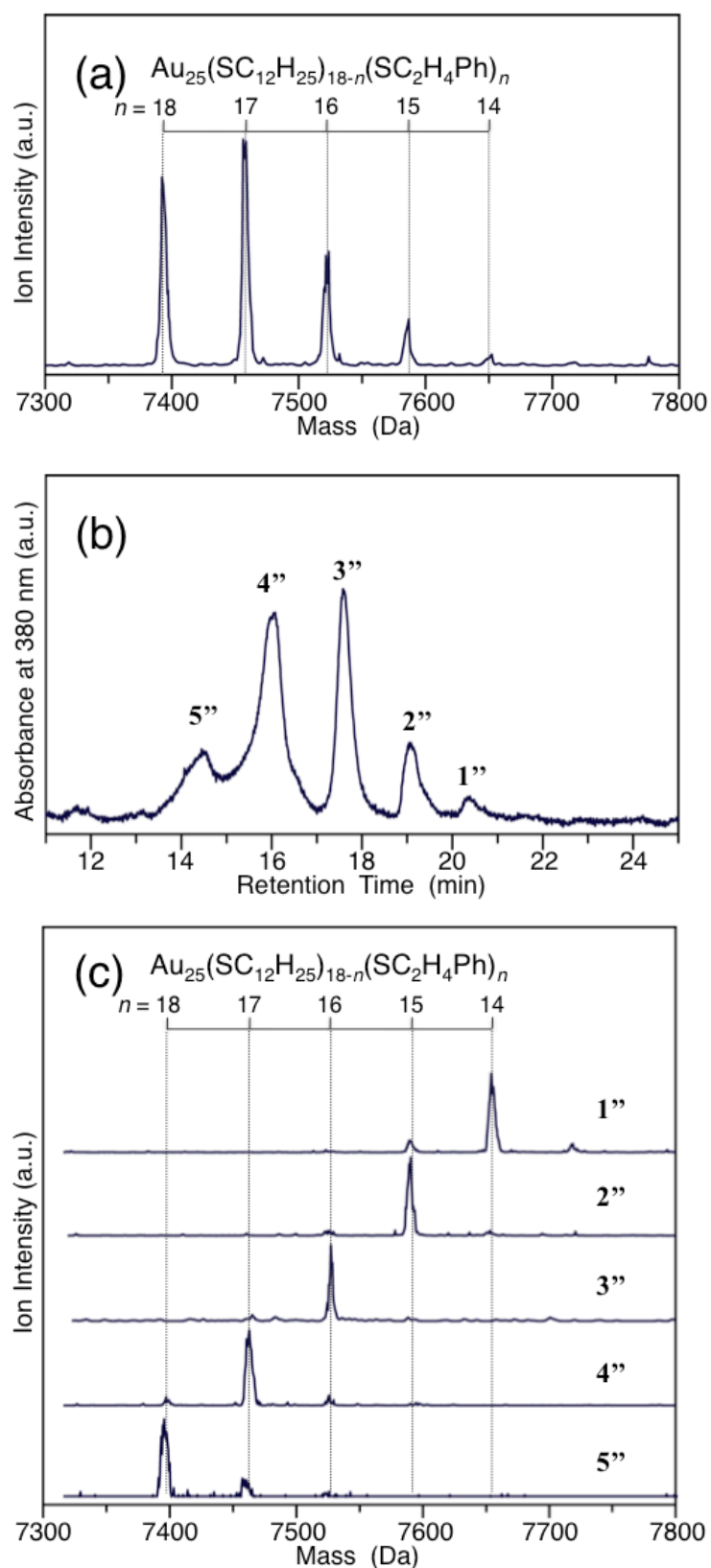


Figure S15. (a) Negative ion MALDI mass spectrum of Au₂₅(SC₁₂H₂₅)_{18-n}(SC₂H₄Ph)_n ($n = 14-18$). (b) chromatogram of these clusters. (c) Negative ion MALDI mass spectra of the fractions of each peak section appeared in the chromatogram, 1''-5''. These results indicate that each peak section, 1''-5'', contains a single Au₂₅(SC₁₂H₂₅)_{18-n}(SC₂H₄Ph)_n in high purity and that Au₂₅(SC₁₂H₂₅)_{18-n}(SC₂H₄Ph)_n clusters were separated at high resolution depending on the chemical composition.

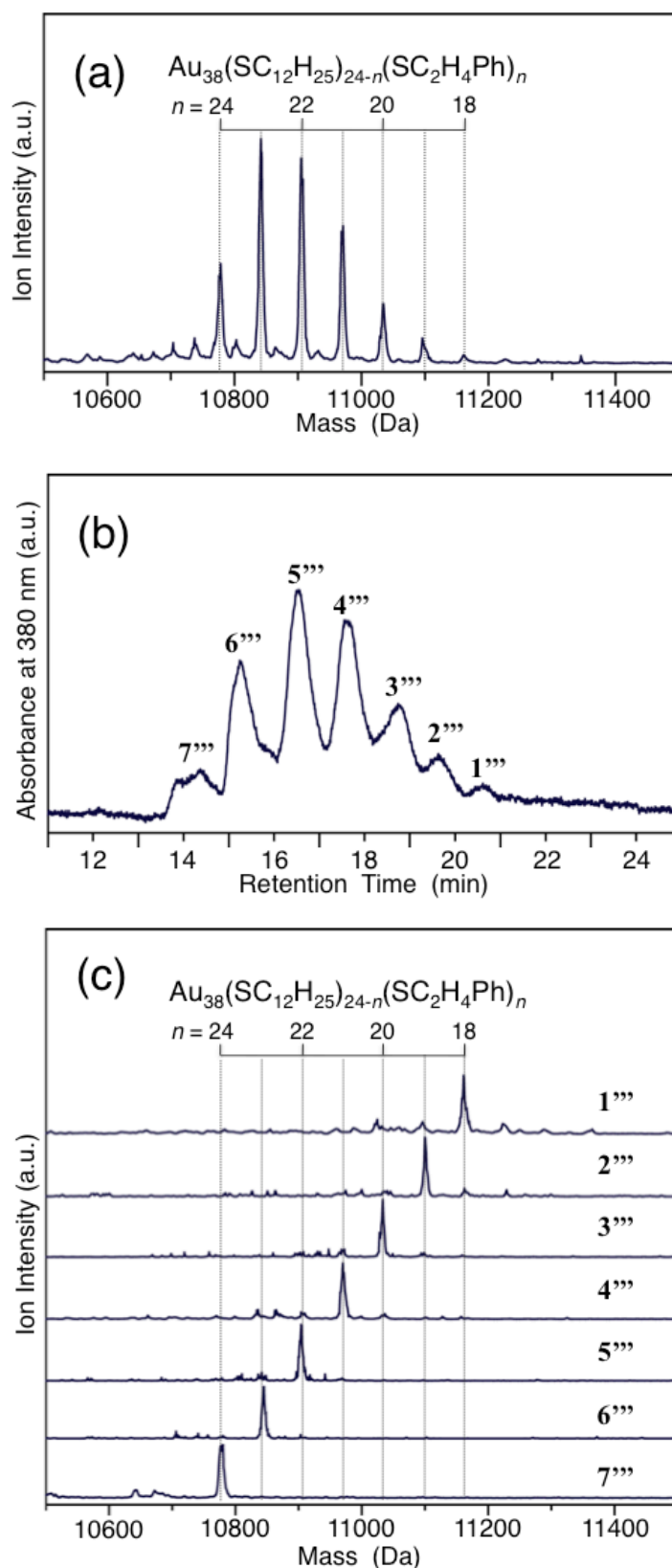


Figure S16. (a) Positive ion MALDI mass spectrum of $\text{Au}_{38}(\text{SC}_{12}\text{H}_{25})_{24-n}(\text{SC}_2\text{H}_4\text{Ph})_n$ ($n = 18-24$). (b) Chromatograms of these clusters. (c) Positive ion MALDI mass spectra of the fractions of each peak appearing in the chromatogram, $1'''-7'''$. These results indicate that each peak, $1'''-7'''$, contains a single $\text{Au}_{38}(\text{SC}_{12}\text{H}_{25})_{24-n}(\text{SC}_2\text{H}_4\text{Ph})_n$ at high purity and that $\text{Au}_{38}(\text{SC}_{12}\text{H}_{25})_{24-n}(\text{SC}_2\text{H}_4\text{Ph})_n$ clusters were separated at high resolution depending on the chemical composition.

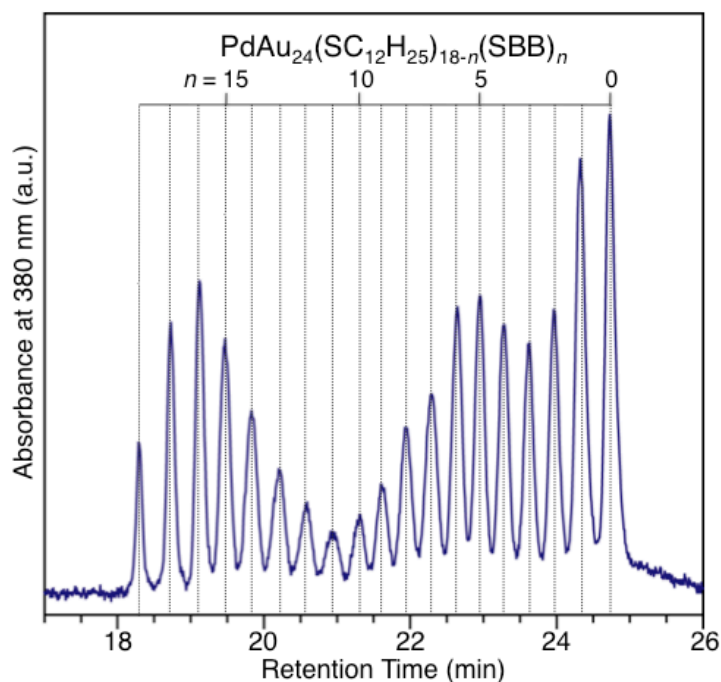


Figure S17. Chromatogram of a mixture of $\text{PdAu}_{24}(\text{SC}_{12}\text{H}_{25})_{18-n}(\text{SBB})_n$ ($n = 0-18$) observed with a mobile phase gradient program different from that used in this work. This gradient program was composed of a combination of a linear line and a curved line. $\text{PdAu}_{24}(\text{SC}_{12}\text{H}_{25})_{18-n}(\text{SBB})_n$ with a broad distribution ($n = 0-18$) was prepared by mixing several $\text{PdAu}_{24}(\text{SC}_{12}\text{H}_{25})_{18-n}(\text{SBB})_n$ clusters with different distributions. In this chromatogram, each peak progresses at nearly regular intervals. This peak pattern is consistent with that observed in the mass spectrum. This makes conformation of the separation of each cluster easy and allows an estimate of the abundance ratio of each cluster.

References

1. Negishi, Y.; Kurashige, W.; Niihori, Y.; Iwasa, T.; Nobusada, K. *Phys. Chem. Chem. Phys.* **2010**, *12*, 6219–6255.
2. Negishi, Y.; Chaki, N. K.; Shichibu, Y.; Whetten, R. L.; Tsukuda, T. *J. Am. Chem. Soc.* **2007**, *129*, 11322–11323.
3. Chaki, N. K.; Negishi, Y.; Tsunoyama, H.; Shichibu, Y.; Tsukuda, T. *J. Am. Chem. Soc.* **2008**, *130*, 8608–8610.
4. Heaven, M. W.; Dass, A.; White, P. S.; Holt, K. M.; Murray, R. W. *J. Am. Chem. Soc.* **2008**, *130*, 3754.
5. Zhu, M.; Aikens, C. M.; Hollander, F. J.; Schatz, G. C.; Jin, R. *J. Am. Chem. Soc.* **2008**, *130*, 5883.
6. Qian, H.; Eckenhoff, W. T.; Zhu, Y.; Pintauer, T.; Jin, R. *J. Am. Chem. Soc.* **2010**, *132*, 8280–8281.
7. Niihori, Y.; Kurashige, W.; Matsuzaki, M.; Negishi, Y. *Nanoscale* **2013**, *5*, 508–512.
8. Dolamic, I.; Knoppe, S.; Dass, A.; Bürgi, T. *Nat. Commun.* **2012**, *3*, 798–803.
9. Knoppe, S.; Azoulay, R.; Dass, A.; Bürgi, T. *J. Am. Chem. Soc.* **2012**, *134*, 20302–20305.
10. Knoppe, S.; Dolamic, I.; Dass, A.; Bürgi, T. *Angew. Chem. Int. Ed.* **2012**, *51*, 7589–7591.
11. Dass, A.; Stevenson, A.; Dubay, G. R.; Tracy, J. B.; Murray, R. W. *J. Am. Chem. Soc.* **2008**, *130*, 5940–5946.